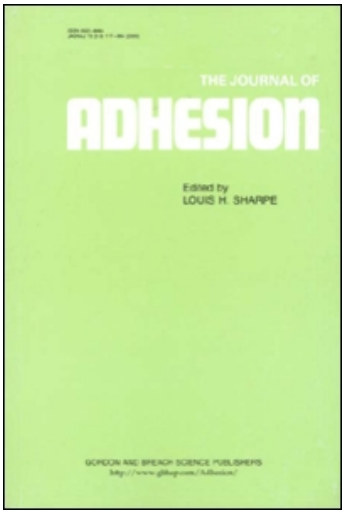

The Journal of Adhesion

Publication details, including instructions for authors and subscription information:
http://www.informaworld.com/smpp/title~content=t713453635

Nonlinear Analysis of theTorque Transmission Capability of Adhesively Bonded Tubular Lap Joints

Dai Gil Lee[a]; Je Hoon Oh[a]
[a] Department of Mechanical Engineering, ME3221, Korea Advanced Institute of Science and Technology, Korea

Online publication date: 02 December 2010

To cite this Article Lee, Dai Gil and Oh, Je Hoon(1999) 'Nonlinear Analysis of theTorque Transmission Capability of Adhesively Bonded Tubular Lap Joints', The Journal of Adhesion, 71: 1, 81 — 106
To link to this Article: DOI: 10.1080/00218469908009567
URL: http://dx.doi.org/10.1080/00218469908009567

J. Adhesion, 1999, Vol. 71, pp. 81–106
Reprints available directly from the publisher
Photocopying permitted by license only

Nonlinear Analysis of the Torque Transmission Capability of Adhesively Bonded Tubular Lap Joints

DAI GIL LEE * and JE HOON OH

Department of Mechanical Engineering, ME3221, Korea Advanced Institute of Science and Technology, Kusong-dong, Yusong-Ku, Taejon-shi, Korea 305-701

(Received 2 January 1999; In final form 2 April 1999)

Calculated torque transmission capability of adhesively bonded tubular lap joints using linear elastic material properties is usually much less than the experimentally-determined one because the majority of the load transfer of the adhesively bonded joints is accomplished by the nonlinear behavior of rubber-toughened epoxy adhesives.

Although the adhesively bonded tubular double lap joint has better torque transmission capability and reliability than the single lap joint, the nonlinear analytic or numerical analysis for the adhesively bonded tubular double lap joint has not been performed because of numerical complications.

An iterative solution that includes the nonlinear shear behavior of the adhesive was derived using the analytic solution. Since the iterative solution can be obtained very quickly due to the simplicity of the algorithm, it is an attractive method of designing adhesively bonded tubular single and double lap joints.

Keywords: Adhesively bonded tubular lap joint; nonlinear shear behavior of adhesive; torque transmission capability; iterative solution

INTRODUCTION

Epoxy adhesives that are toughened by rubber possess nonlinear material properties. The mechanical elements joined by adhesives with nonlinear properties also behave nonlinearly, therefore, the exact solutions are not easily obtained. Most exact solutions of adhesively bonded

*Corresponding author. Tel.: +82 42 869 3002, Fax: +82 42 869-3210, -5210.

joints were only obtained with several assumptions such as linear elastic behavior of the adhesive and the adherend.

Adhesively bonded tubular lap joints are usually divided into two kinds, such as the single-lap joint and the double-lap joint. Numerous studies on adhesively bonded tubular single-lap joints were performed after Adams [1] obtained the elastic solution of the adhesively bonded tubular single-lap joint. The time-dependent viscoelastic behavior of the adhesive was investigated by Alwar and Nagaraja [2]. Hart-Smith performed analyses of several types of adhesively bonded joints such as the single-lap, the double-lap, the scarf and the stepped-lap joint [3]. The behaviors of adhesively bonded joints whose adherends were made of orthotropic materials, such as composites, were investigated by several researchers [4–6]. The effect of the adhesive thickness and the adherend roughness on the torsional fatigue strength of adhesively bonded tubular single lap joints was investigated by Lee *et al.* [7]. They showed that the torsional fatigue strength of the joint increased as the adhesive thickness decreased and the optimal arithmetic surface roughness of the adherend was about 2 μm. Lee and Lee proposed an adhesive failure model of the adhesively bonded tubular single lap joint to predict the torque transmission capability accurately [8]. A method for the optimal design of the adhesively bonded tubular single-lap joint was proposed based on the failure model of the adhesively bonded tubular single-lap joint by Lee and Lee [9]. Choi and Lee investigated the static and dynamic torque transmission capabilities of adhesively bonded polygonal lap joints for carbon fiber epoxy composites [10]. Experimentally, they found that the fatigue strength of circular adhesively bonded joints was dependent on the surface roughness of the adherends and that polygonal adhesively bonded joints had better fatigue strength characteristics than circular adhesively bonded joints. Lee and Lee derived an iterative solution of adhesively bonded tubular single-lap joints which included the nonlinear shear properties of the adhesive [11].

Although the adhesively bonded tubular double-lap joint has generally better torque transmission capability and reliability than the single-lap joint, there have been only a few studies on adhesively bonded tubular double-lap joints in comparison with those on adhesively bonded tubular single-lap joints. The stresses and torque transmission capabilities of the adhesively bonded tubular single- and double-lap

joints were experimentally tested by Choi and Lee [12]. They also performed 3-dimensional finite element analyses taking into consideration the nonlinear properties of the adhesive in order to compare the experimental results with the calculated results. Lee and Lee developed a closed-form solution for the torque transmission capability and stress distribution of the adhesively bonded tubular double-lap joint assuming linear properties of the adhesive [13]. Since adhesively bonded joints generally behave nonlinearly, the simple linear elastic solution of the adhesively bonded tubular double-lap joint underestimates the torque transmission capabilities. If the simple linear elastic solution developed by Adams [1] is used for calculating the shear stress distribution of the adhesive, severe stress concentrations appear at the ends of the adhesive layer. Therefore, the shear stresses at the ends of the adhesive layer calculated by the linear elastic solution arrive at the failure shear strength even though the applied torque is far less than the maximum torque. However, in fact, the high stress concentrations calculated by the linear elastic analysis are relieved to a great extent because of the nonlinear behavior of the adhesive. Thus, in order to obtain the accurate torque transmission capability of the adhesively bonded tubular double-lap joint, the torque transmission capability of the joint should be calculated considering the nonlinear shear behavior of the adhesive. Since an iterative solution for adhesively bonded tubular single-lap joints with nonlinear shear properties of the adhesive developed by Lee *et al.* [11] could not be applied to adhesively bonded tubular double-lap joints, the nonlinear solution for adhesively bonded double-lap joints should be developed.

In this paper, the iterative solution proposed by Lee *et al.* [11] was modified and improved to develop the nonlinear solution for both adhesively bonded single- and double-lap joints. In order to verify the solution, the torque transmission capabilities of adhesively bonded tubular single- and double-lap joints were calculated and compared with the experimental results obtained from the work of one of the authors [8, 12, 14]. The torque transmission capability and stress distribution in the adhesive layer of adhesively bonded tubular double-lap joints were calculated and compared with those of adhesively bonded tubular single-lap joints. Also, the effect of the adherend thickness and adhesive bonding length of the joint on the torque transmission capability was investigated.

Since the iterative solution can be obtained very quickly due to its simple calculation algorithm, it could be used in the design of adhesively bonded tubular single- and double-lap joints.

DERIVATION OF THE NONLINEAR SOLUTION

The iterative solution for torque transmission capability of the adhesively bonded tubular double-lap joint with nonlinear shear properties was derived from the analytic solution with linear shear properties. Figure 1 shows the general geometric configuration of the adhesively bonded tubular double-lap joint.

The first step was based on the formulation procedure of Lee *et al.* [13]. In this formulation, it is assumed that the adherends transfer only the stress component of $\tau_{\theta z}$ and the adhesive transfers only the stress

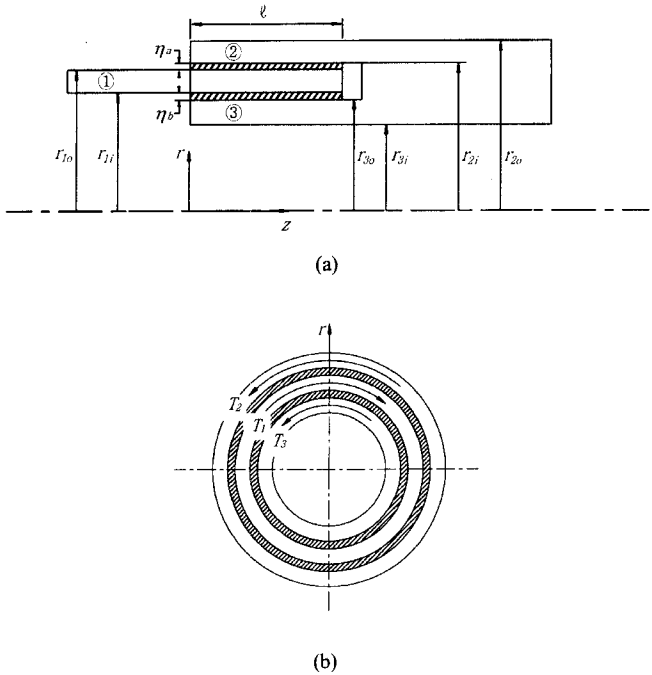

FIGURE 1 Configuration of the adhesively bonded tubular double-lap joint. (a) Shape of the double lap joint, (b) Cross section of the joint.

component of $\tau_{r\theta}$. When the adhesively bonded tubular double-lap joint is subjected to a torque, T, the torques T_1, T_2 and T_3 are produced in the adherends 1, 2 and 3 at any given cross section. Then, from the global equilibrium condition, we have

$$T = T_1 + T_2 + T_3 = \frac{\tau_{1o} J_1}{r_{1o}} + \frac{\tau_{2i} J_2}{r_{2i}} + \frac{\tau_{3o} J_3}{r_{3o}} \tag{1}$$

where r_{1o}, r_{2i} and r_{3o} are the outer radius of the adherend 1, the inner radius of the adherend 2 and the outer radius of the adherend 3, respectively, and J_1, J_2 and J_3 are the polar moments of inertia of the area of the adherends 1, 2 and 3, respectively.

The torque increments of the adherends 1, 2 and 3 in the axial (z) direction were calculated as follows:

$$T_1 + \Delta T_1 - T_1 = -\tau_o(r_{1o}) 2\pi r_{1o}^2 \Delta z - \tau_i(r_{1i}) 2\pi r_{1i}^2 \Delta z \tag{2a}$$

$$T_2 + \Delta T_2 - T_2 = \tau_o(r_{2i}) 2\pi r_{2i}^2 \Delta z \tag{2b}$$

$$T_3 + \Delta T_3 - T_3 = \tau_i(r_{3o}) 2\pi r_{3o}^2 \Delta z \tag{2c}$$

where $\tau_o(r)$ and $\tau_i(r)$ are the shear stresses of the adhesive between the adherends 1 and 2, and between the adherends 1 and 3, respectively.

Since the torque is constant along the adhesive thickness direction ($\tau_i(r) 2\pi r^2 = \tau_i(r_{3o}) 2\pi r_{3o}^2$, $\tau_o(r) 2\pi r^2 = \tau_o(r_{1o}) 2\pi r_{1o}^2$), the stress and strain in the adhesive are highest at the inner part of each adhesive layer along the adhesive thickness. In order to calculate the torque increments in the adhesives at which the stresses are highest, the following equations were derived from Eqs. (2) by applying $\delta z \to 0$.

$$\frac{dT_1}{dz} = -\tau_a 2\pi r_{1o}^2 - \tau_b 2\pi r_{3o}^2 \tag{3a}$$

$$\frac{dT_2}{dz} = \tau_a 2\pi r_{1o}^2 \tag{3b}$$

$$\frac{dT_3}{dz} = \tau_b 2\pi r_{3o}^2 \tag{3c}$$

where τ_a and τ_b are the shear stresses in the adhesive at $r = r_{1o}$ and $r = r_{3o}$, respectively.

Since the adhesive behaves nonlinearly along the adhesive thickness direction, the compatibility conditions for the adhesives and the adherends in an element of the joint of length dz are as follows.

$$\int_{r_{1o}}^{r_{2i}} \gamma_o(r)|_{z+dz}\, dr - \int_{r_{1o}}^{r_{2i}} \gamma_o(r)|_z\, dr = (\gamma_{2i} - \gamma_{1o})\, dz \tag{4a}$$

$$\int_{r_{3o}}^{r_{1i}} \gamma_i(r)|_{z+dz}\, dr - \int_{r_{3o}}^{r_{1i}} \gamma_i(r)|_z\, dr = (\gamma_{3o} - \gamma_{1i})\, dz \tag{4b}$$

where $\gamma_o(r)$ and $\gamma_i(r)$ are the shear strains of the adhesive between the adherends 1 and 2, and between the adherends 1 and 3, respectively, and γ_{1i}, γ_{1o}, γ_{2i} and γ_{3o} are the shear strains in the adherends 1, 2 and 3, respectively.

The integral forms of Eqs. (4) were simplified by introducing non-dimensional weighting factors, w_a and w_b, as follows.

$$\int_{r_{1o}}^{r_{2i}} \gamma_o(r)|_z\, dr = w_a \gamma_a \eta_a \tag{5a}$$

$$\int_{r_{3o}}^{r_{1i}} \gamma_i(r)|_z\, dr = w_b \gamma_b \eta_b \tag{5b}$$

$$\begin{aligned}\int_{r_{1o}}^{r_{2i}} \gamma_o(r)|_{z+dz}\, dr &= (w_a + dw_a)\cdot(\gamma_a + d\gamma_a)\eta_a \\ &= (w_a\gamma_a + w_a d\gamma_a + \gamma_a dw_a + dw_a d\gamma_a)\eta_a \\ &\approx (w_a\gamma_a + w_a d\gamma_a + \gamma_a dw_a)\eta_a \quad (\because dw_a d\gamma_a \approx 0)\end{aligned} \tag{5c}$$

$$\begin{aligned}\int_{r_{3o}}^{r_{1i}} \gamma_i(r)|_{z+dz}\, dr &= (w_b + dw_b)\cdot(\gamma_b + d\gamma_b)\eta_b \\ &= (w_b\gamma_b + w_b d\gamma_b + \gamma_b dw_b + dw_b d\gamma_b)\eta_b \\ &\approx (w_b\gamma_b + w_b d\gamma_b + \gamma_b dw_b)\eta_b \quad (\because dw_b d\gamma_b \approx 0)\end{aligned} \tag{5d}$$

where γ_a and γ_b are the shear strains in the adhesive at $r = r_{1o}$ and $r = r_{3o}$, respectively, and η_a and η_b are the adhesive thicknesses of each layer defined as follows:

$$\eta_a = r_{2i} - r_{1o} \tag{6a}$$

$$\eta_b = r_{1i} - r_{3o} \tag{6b}$$

Substituting Eqs. (5) into Eqs. (4), the following equations were obtained.

$$\frac{d\gamma_a}{dz} = \frac{\gamma_{2i} - \gamma_{1o}}{w_a \eta_a} - \frac{dw_a}{dz}\frac{\gamma_a}{w_a} \tag{7a}$$

$$\frac{d\gamma_b}{dz} = \frac{\gamma_{3o} - \gamma_{1i}}{w_b \eta_b} - \frac{dw_b}{dz}\frac{\gamma_b}{w_b} \tag{7b}$$

Since the adhesive in general behaves nonlinearly due to rubber toughening, while the adherend used in joining operations behaves linearly, in this paper the adherends are assumed to behave linear elastically. Also, it is assumed that mechanical strains due to the applied torque are large compared with the creep strains at the normal loading rate, and all nonlinear time and temperature dependent effects are negligible. Under such assumptions, the shear stress in the adhesive was represented by a function of the shear strain in the adhesive.

$$\tau_a = f(\gamma_a) \tag{8a}$$

$$\tau_b = f(\gamma_b) \tag{8b}$$

Since the torque is constant along the adhesive thickness direction, the weighting factors, w_a and w_b, were calculated by using Eqs. (8).

$$w_a = \frac{\int_{r_{1o}}^{r_{2i}} \gamma_o(r)|_z dr}{\gamma_a \eta_a} = \frac{\int_{r_{1o}}^{r_{2i}} f^{-1}\left(\frac{r_{1o}^2}{r^2}\tau_a\right) dr}{\gamma_a \eta_a} \tag{9a}$$

$$w_b = \frac{\int_{r_{3o}}^{r_{1i}} \gamma_i(r)|_z dr}{\gamma_b \eta_b} = \frac{\int_{r_{3o}}^{r_{1i}} f^{-1}\left(\frac{r_{3o}^2}{r^2}\tau_b\right) dr}{\gamma_b \eta_b} \tag{9b}$$

From Eqs. (8), the shear stress increments of the adhesive with respect to the shear strain increment were expressed as follows:

$$d\tau_a = \frac{df(\gamma_a)}{d\gamma_a} d\gamma_a \tag{10a}$$

$$d\tau_b = \frac{df(\gamma_b)}{d\gamma_b} d\gamma_b \tag{10b}$$

Differentiating Eqs. (3) with respect to z and using Eqs. (7) and (10), the following equations were derived.

$$\frac{d^2T_2}{dz^2} = 2\pi r_{1o}^2 \frac{df(\gamma_a)}{d\gamma_a} \left(\frac{\gamma_{2i} - \gamma_{1o}}{w_a \eta_a} - \frac{dw_a}{dz} \frac{\gamma_a}{w_a} \right) \tag{11a}$$

$$\frac{d^2T_3}{dz^2} = 2\pi r_{3o}^2 \frac{df(\gamma_b)}{d\gamma_b} \left(\frac{\gamma_{2o} - \gamma_{1i}}{w_b \eta_b} - \frac{dw_b}{dz} \frac{\gamma_b}{w_b} \right) \tag{11b}$$

Differentiating T_2 and T_3 in Eq. (1) twice with respect to z and using the results of Eqs. (11) with elastic relationships of the adherends ($\gamma_{1o} = (\tau_{1o}/G_1)$, $\gamma_{2i} = (\tau_{2i}/G_2)$ and $\gamma_{3o} = (\tau_{3o}/G_3)$), the following equations were derived.

$$\frac{d^2\tau_{2i}}{dz^2} = 2\pi r_{1o}^2 \frac{df(\gamma_a)}{d\gamma_a} \frac{r_{2i}}{w_a J_2} \left\{ \frac{1}{\eta_a} \left(\frac{\tau_{2i}}{G_2} - \frac{\tau_{1o}}{G_1} \right) - \frac{dw_a}{dz} \gamma_a \right\} \tag{12a}$$

$$\frac{d^2\tau_{3o}}{dz^2} = 2\pi r_{3o}^2 \frac{df(\gamma_b)}{d\gamma_b} \frac{r_{3o}}{w_b J_3} \left\{ \frac{1}{\eta_b} \left(\frac{\tau_{3o}}{G_3} - \frac{\tau_{1i}}{G_1} \right) - \frac{dw_b}{dz} \gamma_b \right\} \tag{12b}$$

From Eq. (1), τ_{1o} and τ_{1i} were expressed as follows.

$$\tau_{1o} = \frac{r_{1o}}{J_1} \left(T - \frac{\tau_{2i} J_2}{r_{2i}} - \frac{\tau_{3o} J_3}{r_{3o}} \right) \tag{13a}$$

$$\tau_{1i} = \frac{r_{1i}}{J_1} \left(T - \frac{\tau_{2i} J_2}{r_{2i}} - \frac{\tau_{3o} J_3}{r_{3o}} \right) \tag{13b}$$

Substituting Eqs. (13) into Eqs. (12), the second order differential equations with nonlinear properties of the adhesive were derived as follows:

$$\frac{d^2\tau_{2i}}{dz^2} = 2\pi r_{1o}^2 \frac{df(\gamma_a)}{d\gamma_a}\frac{r_{2i}}{w_a J_2}\left(\frac{1}{\eta_a G_2} + \frac{r_{1o}J_2}{\eta_a G_1 J_1 r_{2i}}\right)\tau_{2i} - 2\pi r_{1o}^2 \frac{df(\gamma_a)}{d\gamma_a}\frac{r_{2i}}{w_a J_2}\left(\frac{r_{1o}T}{\eta_a G_1 J_1} + \frac{dw_a}{dz}\gamma_a\right) + 2\pi r_{1o}^2 \frac{df(\gamma_a)}{d\gamma_a}\frac{r_{2i}}{w_a J_2}\frac{r_{1o}J_3}{\eta_a G_1 J_1 r_{3o}}\tau_{3o} \tag{14a}$$

$$\frac{d^2\tau_{3o}}{dz^2} = 2\pi r_{3o}^2 \frac{df(\gamma_b)}{d\gamma_b}\frac{1}{w_b\eta_b}\left(\frac{r_{3o}}{G_3 J_3} + \frac{r_{1i}}{G_1 J_1}\right)\tau_{3o} - 2\pi r_{3o}^2 \frac{df(\gamma_b)}{d\gamma_b}\frac{r_{3o}}{w_b J_3}\left(\frac{r_{1i}T}{\eta_b G_1 J_1} + \frac{dw_b}{dz}\gamma_b\right) + 2\pi r_{3o}^2 \frac{df(\gamma_b)}{d\gamma_b}\frac{r_{3o}}{w_b J_3}\frac{r_{1i}J_2}{\eta_b G_1 J_1 r_{2i}}\tau_{2i} \tag{14b}$$

Eqs. (14) can be simplified as follows:

$$\frac{d^2\tau_{2i}}{dz^2} = \alpha_1(\gamma_a)\tau_{2i} + \alpha_2(\gamma_a) + \alpha_3(\gamma_a)\tau_{3o} \tag{15a}$$

$$\frac{d^2\tau_{3o}}{dz^2} = \alpha_4(\gamma_b)\tau_{3o} + \alpha_5(\gamma_b) + \alpha_6(\gamma_b)\tau_{2i} \tag{15b}$$

where

$$\alpha_1 = 2\pi r_{1o}^2 \frac{df(\gamma_a)}{d\gamma_a}\frac{1}{w_a\eta_a}\left(\frac{r_{2i}}{G_2 J_2} + \frac{r_{1o}}{G_1 J_1}\right)$$

$$\alpha_2 = -2\pi r_{1o}^2 \frac{df(\gamma_a)}{d\gamma_a}\frac{r_{2i}}{w_a J_2}\left(\frac{r_{1o}T}{\eta_a G_1 J_1} + \frac{dw_a}{dz}\gamma_a\right)$$

$$\alpha_3 = 2\pi r_{1o}^2 \frac{df(\gamma_a)}{d\gamma_a}\frac{r_{2i}}{w_a J_2}\frac{r_{1o}J_3}{\eta_a G_1 J_1 r_{3o}}$$

$$\alpha_4 = 2\pi r_{3o}^2 \frac{df(\gamma_b)}{d\gamma_b}\frac{1}{w_b\eta_b}\left(\frac{r_{3o}}{G_3 J_3} + \frac{r_{1i}}{G_1 J_1}\right)$$

$$\alpha_5 = -2\pi r_{3o}^2 \frac{df(\gamma_b)}{d\gamma_b}\frac{r_{3o}}{w_b J_3}\left(\frac{r_{1i}T}{\eta_b G_1 J_1} + \frac{dw_b}{dz}\gamma_b\right)$$

$$\alpha_6 = 2\pi r_{3o}^2 \frac{df(\gamma_b)}{d\gamma_b}\frac{r_{3o}}{w_b J_3}\frac{r_{1i}J_2}{\eta_b G_1 J_1 r_{2i}}$$

The boundary conditions at the joint edges were,

$$\tau_{2i} = 0 \quad \text{and} \quad \tau_{3o} = 0 \quad \text{at} \quad z = 0 \tag{16a}$$

$$\tau_{2i} = \frac{r_{2i}T}{J_2 + J_3} \quad \text{and} \quad \tau_{3o} = \frac{r_{3o}T}{J_2 + J_3} \quad \text{at} \quad z = \ell \tag{16b}$$

Eqs. (15) can be rewritten in the iterative form as shown below.

$$\frac{d^2\tau_{2i}^{(i+1)}}{dz^2} = \alpha_1^{(i)}(\gamma_a^{(i)})\tau_{2i}^{(i+1)} + \alpha_2^{(i)}(\gamma_a^{(i)}) + \alpha_3^{(i)}(\gamma_a^{(i)})\tau_{3o}^{(i+1)} \tag{17a}$$

$$\frac{d^2\tau_{3o}^{(i+1)}}{dz^2} = \alpha_4^{(i)}(\gamma_b^{(i)})\tau_{3o}^{(i+1)} + \alpha_5^{(i)}(\gamma_b^{(i)}) + \alpha_6^{(i)}(\gamma_b^{(i)})\tau_{2i}^{(i+1)} \tag{17b}$$

The parameters $\alpha_j^{(i)}$, $j = 1-6$ in Eqs. (17) represent the functions of strains of the adhesive during the i-th iteration. To obtain the values of parameters of the current step, the strains of the adhesive of the previous step were used. To solve the boundary value problem, it was converted into an equivalent initial value problem. The fourth-order Runge-Kutta method and the shooting method were used to solve the system of the initial value problems.

$$\begin{aligned}
\frac{d\tau_{2i}^{(i+1)}}{dz} &= X^{(i+1)} \\
\frac{dX^{(i+1)}}{dz} &= \alpha_1^{(i)}(\gamma_a^{(i)})\tau_{2i}^{(i+1)} + \alpha_2^{(i)}(\gamma_a^{(i)}) + \alpha_3^{(i)}(\gamma_a^{(i)})\tau_{3o}^{(i+1)} \\
\frac{d\tau_{3o}^{(i+1)}}{dz} &= Y^{(i+1)} \\
\frac{dY^{(i+1)}}{dz} &= \alpha_4^{(i)}(\gamma_b^{(i)})\tau_{3o}^{(i+1)} + \alpha_5^{(i)}(\gamma_b^{(i)}) + \alpha_6^{(i)}(\gamma_b^{(i)})\tau_{2i}^{(i+1)}
\end{aligned} \tag{18}$$

After the shear stress distributions at the inner surface of the adherend 2 and at the outer surface of the adherend 3 were obtained from Eq. (18), the shear stress distributions at the inner surface and the outer surface of the adherend 1 were calculated using Eqs. (13). Also, the shear stress distributions of the adhesive were computed as follows:

$$\tau_a = \frac{J_2}{2\pi r_{1o}^2 r_{2i}} \frac{d\tau_{2i}}{dz} \tag{19a}$$

$$\tau_b = \frac{J_3}{2\pi r_{3o}^3} \frac{d\tau_{3o}}{dz} \tag{19b}$$

Equations (18) become the iterative equation for the adhesively bonded tubular single-lap joint developed by Lee *et al.* [11] in the case of $\tau_{3o} = \alpha_4 = \alpha_5 = \alpha_6 = 0$. Therefore, the nonlinear solutions for both the single- and double-lap joints can be obtained using Eq. (18).

NONLINEAR SHEAR STRESS-SHEAR STRAIN RELATIONS

In order to calculate the torque transmission capability of the joint using the iterative solution, the nonlinear shear behavior of the adhesive should be investigated first. Sancaktar [18] reviewed the characteristics of structural adhesives such as constitutive relations and common testing procedures. The deformation theory, its modification, linear viscoelasticity, time-temperature superposition, nonlinear viscoelasticity, overstress theory, and empirical description of creep behavior were reviewed systematically. Simple power function type relations may be utilized in an empirical fashion to describe the nonlinear behavior of structural adhesives in tensile and shear modes when their mechanical behavior is relatively rate insensitive. When the stress-strain curve has a well-defined initial elastic region, a bi-modal relation can be utilized. Jozavi *et al.* [19] investigated an analytical method of defining and calculating the stress-whitening stress and strain. The analytical relation consisted of a modified bi-linear form of the Ramberg-Osgood equation used in conjunction with bulk tensile data. The effect of stress whitening on the moisture diffusion rate and concentration in a polymer adhesive containing a secondary phase were investigated by Sancaktar *et al.* [20]. They also used a modified bi-linear form of the Ramberg-Osgood equation to model the stress-whitening phenomenon. The torque transmission capability and shear stress distribution of the tubular single lap joint using the nonlinear shear properties of the adhesive were investigated by the first author of this paper [14]. The nonlinear shear properties were represented by the three different mathematical models such as two-parameter exponential,

elastic perfectly-plastic and multilinear strain-softening approximations. They showed that all of the three nonlinear approximations accurately predicted the torque transmission capabilities with an error of less than 5%, from which the two-parameter exponential approximation gave the best prediction. They also showed that the shear stress-strain curves represented by the two-parameter exponential approximation agreed well with the experimentally-determined stress-strain curves for the IPCO 9923 and FM-300 film adhesive. The two-parameter stress-strain curve can be determined when the two material properties such as the initial shear modulus and the ultimate shear strength are known. The equation does not require the determination of the elastic limit of the shear strain. Since the two-parameter exponential approximation method not only gives better prediction but also has the simpler form to be used in the numerical calculation, it has been used in several researches [11, 14–17].

As shown in Eqs. (8) and (15), only the shear stress-shear strain relation of the adhesive is required to obtain the solution. In this work, it is assumed that mechanical strains due to the applied torque are large compared with the creep strains at the normal loading rate, and all nonlinear time and temperature dependent effects are negligible. Considering the accuracy of the result and the simplicity of the constitutive equation, the two-parameter exponential approximation [14] was used as the nonlinear shear properties of the adhesive.

$$\tau = f(\gamma) = \tau_f \left\{ 1 - \exp\left(-\frac{G_a}{\tau_f} \gamma \right) \right\} \tag{20}$$

where τ_f and G_a are the shear strength and initial shear modulus of the adhesive, respectively.

The adhesive used in this example was IPCO 9923, a rubber-toughened epoxy adhesive manufactured by Imperial Polychemicals Corporation (Azusa, California, USA). The shear strength and initial shear modulus of the adhesive were 30 MPa and 0.46 GPa, respectively, and the failure shear strain of the adhesive was 0.4. The experimental shear stress-shear strain curve and Eq. (20) used in the iterative solution are shown in Figure 2. As shown in Figure 2, the exponential model agreed well with the experimental data.

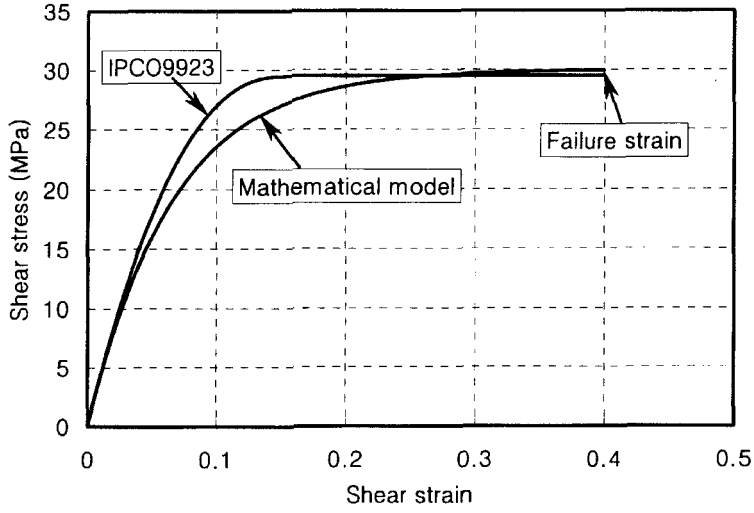

FIGURE 2 Shear stress-shear strain relation of the typical rubber-toughened adhesive.

VERIFICATION OF THE ITERATIVE SOLUTION

In order to verify validity of the iterative solution, the torque transmission capabilities of adhesively bonded tubular single- and double-lap joints calculated with nonlinear properties were compared with the experimental results obtained from the previous works of the first author [8, 12, 14]. The maximum shear strain criterion was used for the adhesive failure and the adherends were assumed not to be failed. Table I shows the geometric configuration of the joints and mechanical properties used for verification.

In the previous experimental works [8, 12, 14], the adhesive bonding thickness of 0.1 mm was chosen and the overlap layers of adherends were abraded by abrasive papers to obtain the arithmetic surface roughness of 2 μm, because these values were suggested for the optimum fatigue strength of the same specimen. Both the inner and outer adherends have accurately ground surfaces, and the concentricity between the outer and inner adherends was secured by mounting the ground surfaces on an accurate V-block during the cure of the adhesive. The specimens were cured in an autoclave under a temperature of 80°C and pressure of 0.6 MPa for 3 hours.

TABLE I Configurations of the adhesively bonded tubular single- and double-lap joints tested in Refs. [8, 12, 14]

	Single-lap joint (Ref. [8])	*Single-lap joint (Ref. [14])*	*Double-lap joint (Ref. [12])*	
			Inner layer	*Outer layer*
r_{1i} (mm)	0	0	8.5	
r_{1o} (mm)	8.4	8.4	10.5	
r_{2i} (mm)	8.5	8.5	10.6	
r_{2o} (mm)	10.5	10.5	12.1	
r_{3i} (mm)	–	–	0	
r_{3o} (mm)	–	–	8.4	
η (mm)	0.1	0.1	0.1	0.1
ℓ (mm)	15.0	10.0	10.0	10.0
G_1, G_2, G_3 (GPa)	80.8	80.8	80.8	
τ_f (MPa)	30.0	30.0	30.0	
G_a (GPa)	0.46	0.46	0.46	

TABLE II Comparison of the torque transmission capability calculated by the present method and measured by the static torsion test (Refs. [8, 12, 14])

	Measured data	*Present method*	*Error (%)*
Single-lap joint (Ref. [8])	190 Nm	191 Nm	0.53
Single-lap joint (Ref. [14])	128 Nm	130 Nm	1.56
Double-lap joint (Ref. [12])	302 Nm	304 Nm	0.66

Table II shows the maximum torque transmission capabilities both experimentally measured and calculated using the iterative solution. From Table II, it was found that the iterative solution accurately predicted the torque transmission capabilities of the adhesively bonded tubular lap joints with an error of less than 2%.

NUMERICAL APPLICATIONS OF THE ITERATIVE SOLUTION

Table III shows the selected geometric configuration of the joints that were used to investigate the effects of the nonlinear shear properties of the adhesive and the adherend thickness on the torque transmission capabilities and the shear stress distributions. It was assumed that the

TABLE III Simulation conditions of the adhesively bonded tubular single- and double-lap joints

	Single-lap joint	*Double-lap joint*	
		Inner layer	*Outer layer*
r_{1i} (mm)	15.0	15.0	
r_{1o} (mm)	18.0	18.0	
r_{2i} (mm)	–	18.1	
r_{2o} (mm)	–	21.1	
r_{3i} (mm)	11.9	11.9	
r_{3o} (mm)	14.9	14.9	
η (mm)	0.1	0.1	0.1
l (mm)	20.0	20.0	20.0
G_1, G_2, G_3 (GPa)	80.8	80.8	
Shear strength of the adhesive (MPa)	30.0	30.0	
Failure strain of the adhesive	0.4	0.4	

adherends were not failed and the maximum shear strain criterion was applied to the adhesive, in order to investigate the effect of nonlinear shear properties on the shear stress and strain distributions in the adhesive layer. The configuration of the single-lap joint was selected to be the same as that of the double-lap joint except that the outer adherend 2 was removed from the double-lap joint as shown in Figure 3.

In general, more than ten minutes were required with an IBM personal computer to obtain the solution by a two-dimensional finite element method with 8-node, axisymmetric-isoparametric elements even though relatively coarse meshes were employed in the axial direction [8, 11]. However, it was found that, through the numerical calculation with the iterative method, both the torque transmission capabilities and the shear stress and strain distributions of the adhesively bonded tubular single- and double-lap joint were calculated within a few to ten seconds due to its simple calculation algorithm.

Figure 4 shows the weighting factors (w_a and w_b) that depend on the joint size and the shear stress at the inner surface of each adhesive layer. The weighting factors decreased rapidly as the shear stress in the adhesive approached the shear strength, and also decreased as the adhesive thickness increased. From Figure 4, it was found that as the shear stress in the adhesive and the adhesive thickness increased, the nonlinear behavior in the adhesive thickness direction increased.

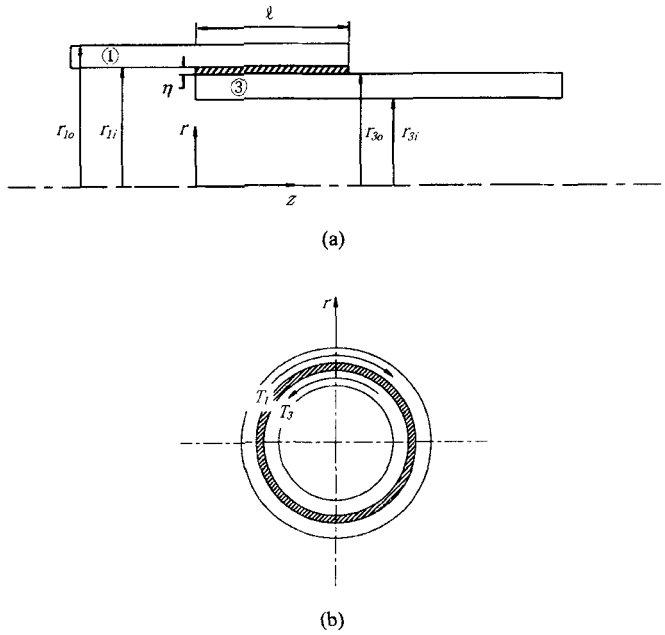

FIGURE 3 Configuration of the adhesively bonded tubular single-lap joint. (a) Shape of the single lap joint, (b) Cross section of the joint.

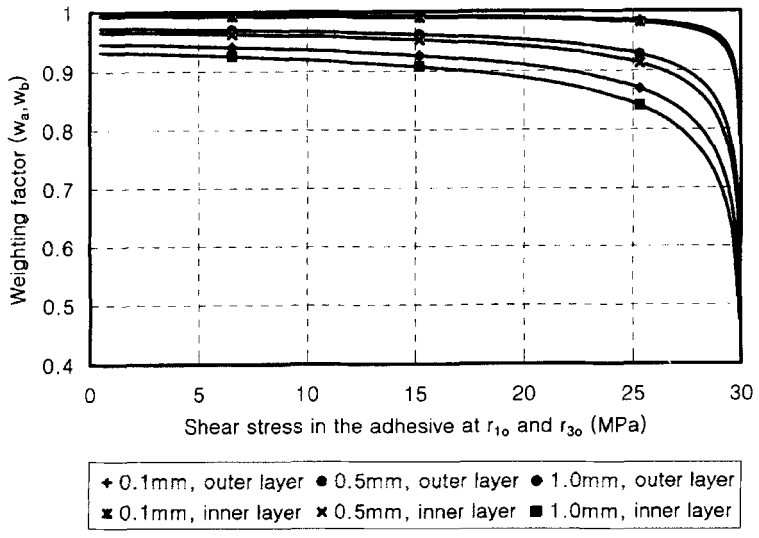

FIGURE 4 Weighting factors of the inner layer and the outer layer w.r.t. the shear stress in the adhesive at r_{1o} and r_{3o} when the adhesive thickness is 0.1 mm, 0.5 mm, and 1.0 mm.

The torque transmission capabilities of the adhesively bonded tubular single- and double-lap joints with respect to the maximum shear strain of the adhesive are shown in Figure 5. The torque transmission capabilities showed nonlinear behavior similar to the shear stress-shear strain curve in Figure 2. As shown in Figure 5, the torque transmission capabilities of the adhesively bonded single-lap joint were almost the same as those calculated by Lee *et al.* [11]. The maximum torque transmission capabilities of the joint with the dimensions in Table III are presented in Table IV. The torque transmission capability of the double-lap joint was improved 86%, compared with that of the single-lap joint.

Since the adhesive thickness is usually small, it has been assumed by many researchers [1, 5, 13, 14] that the shear stress and strain are constant through the thickness of adhesive, consequently, the effect of adhesive thickness is neglected. The same result is obtained if the weighting factors are unity. However, as shown in Figure 5, the torque transmission capabilities were almost same regardless of variation of

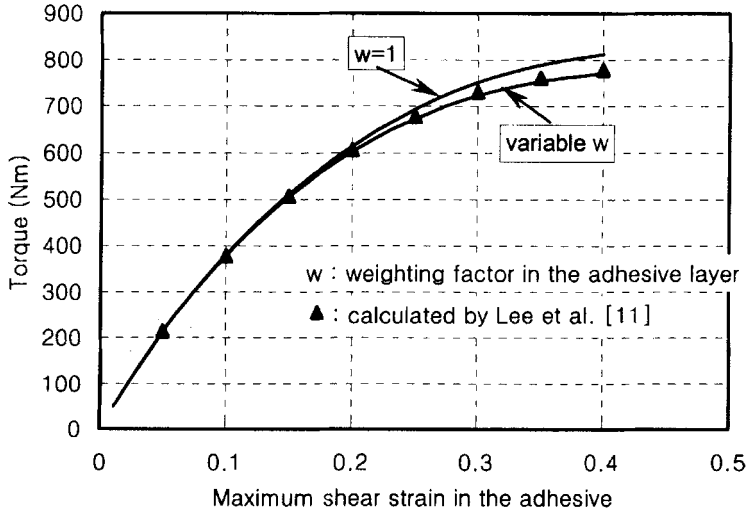

(a)

FIGURE 5 Torque transmission capabilities of the adhesively bonded tubular lap joint w.r.t. the maximum shear strain of the adhesive: (a) Tubular single-lap joint, (b) Tubular double-lap joint.

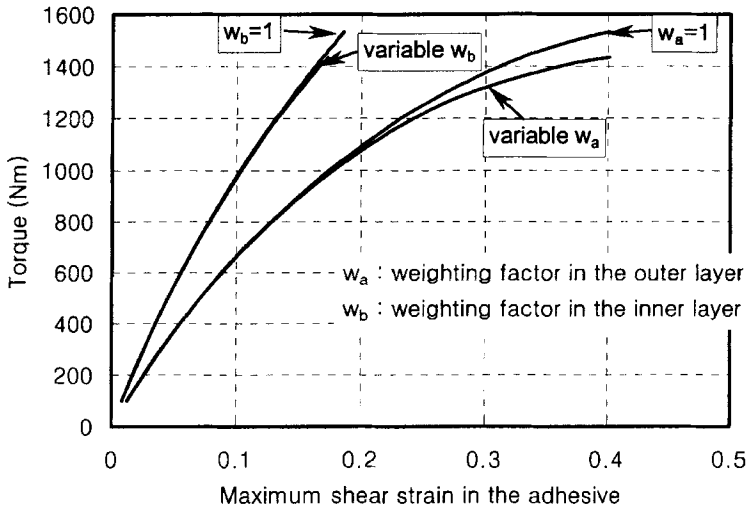

(b)

FIGURE 5 (Continued).

TABLE IV Calculated torque transmission capabilities of the adhesively bonded tubular single- and double-lap joints

	Single-lap joint	*Double-lap joint*	*Note*
Torque transmission capability	771 Nm	1434 Nm	86% improved

the weighting factors when the maximum shear strain of the adhesive was lower than 0.2, while the torque transmission capabilities with the varying weighting factor were lower than those with the constant weighting factor of unity when the maximum shear strain of the adhesive was greater than 0.2. The reason is that as the value of shear strain increases, which requires the use of a varying weighting factor, the nonlinearity of the adhesive along the thickness direction increases. Therefore, the variation of the weighting factors due to the shear stress and strain of the adhesive should be considered to obtain accurate torque transmission capabilities.

Since the outer adhesive layer had the larger maximum shear strain than the inner adhesive layer under the same torque, the outer

adhesive layer was expected to fail before the inner adhesive layer. If failure of the outer adhesive layer has occurred, the applied torque is now supported by the inner adhesive layer only; this has the same configuration as the adhesively bonded single-lap joint. Therefore, it was expected that the failures of the inner and outer adhesive layer occurred simultaneously, because the torque transmission capability of the adhesively bonded tubular single-lap joint was lower than that of the adhesively bonded tubular double-lap joint.

Figure 6 shows the shear stress distributions in the adhesive of the adhesively bonded tubular single- and double-lap joints with respect to applied torque. Both edges of the joints had the highest shear stress and the stress relaxation due to the nonlinear behavior of the adhesive was observed at the ends of the adhesive layers when the shear stresses of the adhesives were high.

The torque transmission capabilities with respect to the thicknesses of the adherend 2 and the adherend 3 are shown in Figure 7, when the thicknesses of the adherend 1 were 2, 3 and 4 mm. The material

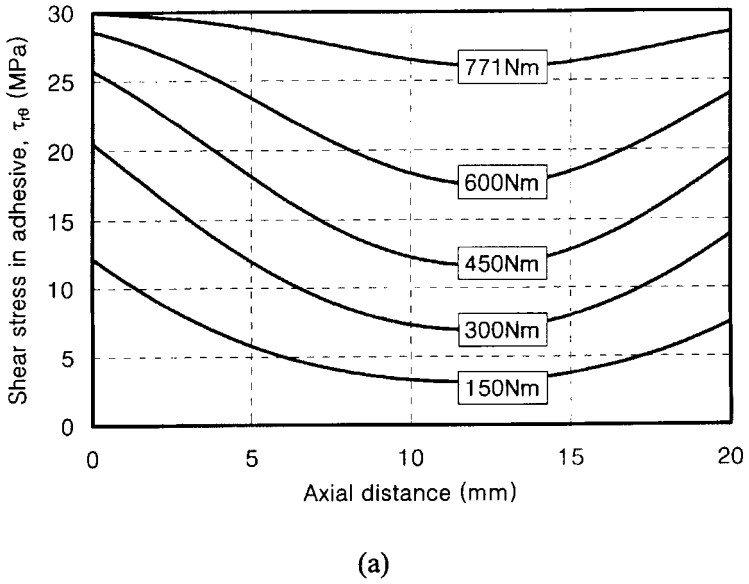

(a)

FIGURE 6 Shear stress distributions in the adhesive w.r.t. the applied torque: (a) Tubular single-lap joint, (b) Outer layer of the tubular double-lap joint, (c) Inner layer of the tubular double-lap joint.

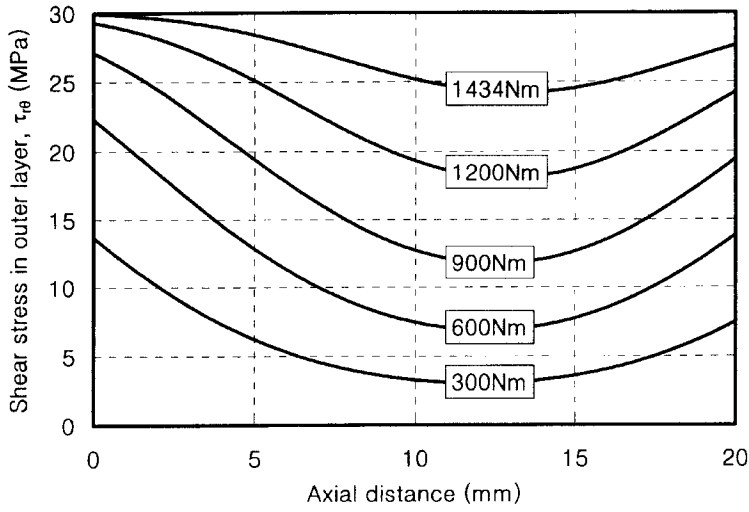

(b)

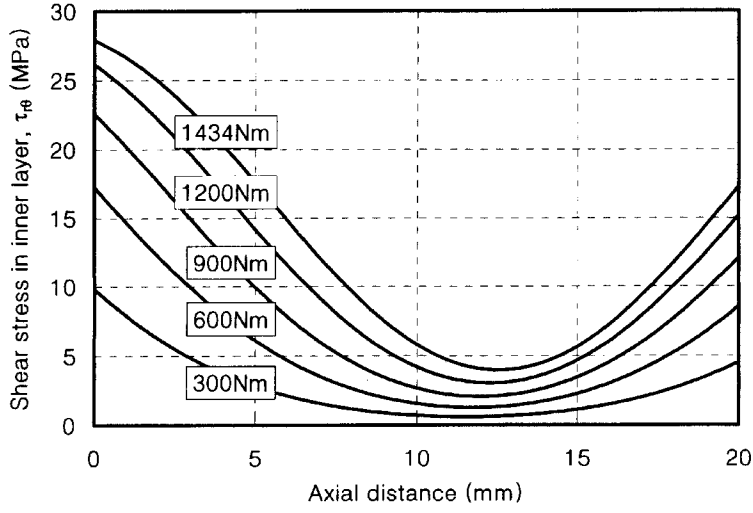

(c)

FIGURE 6 (Continued).

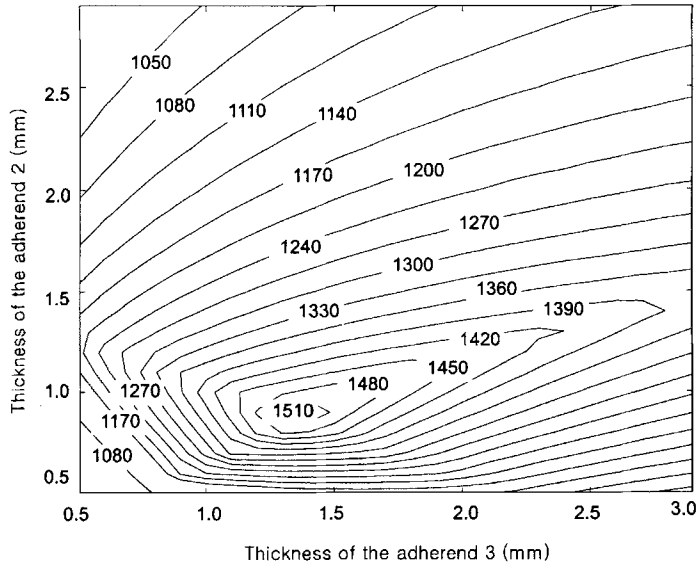

(a)

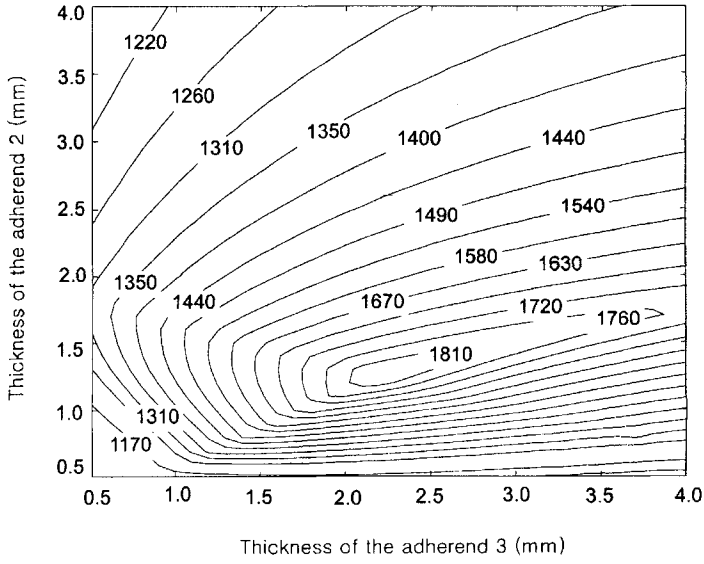

(b)

FIGURE 7 Distributions of the torque transmission capabilities w.r.t. the thickness of the adherends 2 and 3 when the thickness of the adherend 1 is (a) 2 mm (b) 3 mm and (c) 4 mm.

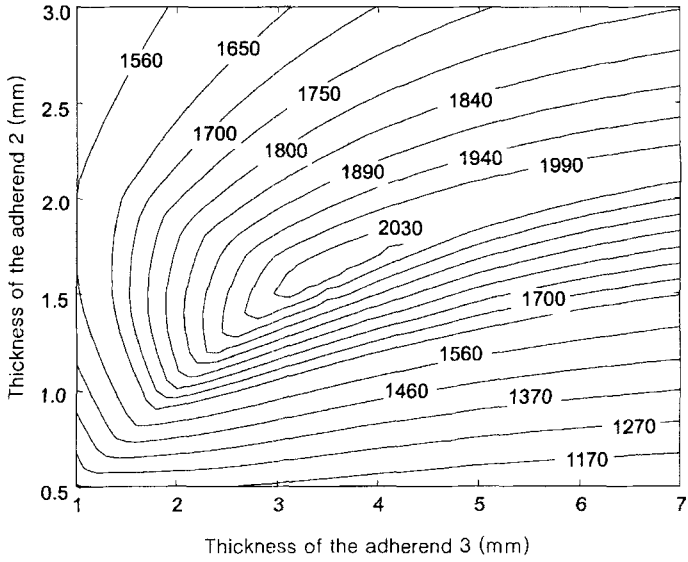

(c)

FIGURE 7 (Continued).

TABLE V Configuration of the adhesively bonded tubular double-lap joint for the maximum torque transmission capability

Thickness of the adherend 1 (mm)	2.00	3.00	4.00
Thickness of the adherend 2 (mm)	0.88	1.26	1.60
Thickness of the adherend 3 (mm)	1.35	2.23	3.38
J_1 (10^{-8} m^4)	5.17	8.54	12.52
J_2 (10^{-8} m^4)	2.98	5.20	7.94
J_3 (10^{-8} m^4)	2.45	3.69	4.97
Torque (Nm)	1551	1867	2086

properties in Table III were used to calculate the torque transmission capabilities. The configuration of the adhesively bonded tubular double-lap joint which gave the maximum torque transmission capability is shown in Table V. From Figure 7, it was found that the maximum torque transmission capability was obtained irrespective of the adherend thickness when the relationship of the adherend polar moments of inertia $J_1 = J_2 + J_3$ was satisfied approximately.

Figure 8 shows the shear stress distribution in the adhesive of the adhesively bonded tubular double-lap joint for the maximum torque transmission capability with respect to the applied torque when the thickness of adherend 1 is 3 mm. As shown in Figure 8, the distributions of shear stresses were symmetric and the magnitudes of shear stresses in the inner and outer adhesive layers were almost the same. From Figure 8, it was found that an efficiently designed adhesively bonded tubular double-lap joint should have the symmetric distribution of the shear stress, and the magnitudes of shear stresses in the inner and outer adhesive layers should be the same, which could be accomplished by adjusting the thickness of the inner and outer female adherends.

The torque transmission capabilities of the two different adhesively tubular double-lap joints with respect to the bonding length are shown in Figure 9, in which the first joint had the same adherend thicknesses of Table V, while the second joint had the same adherend thickness of

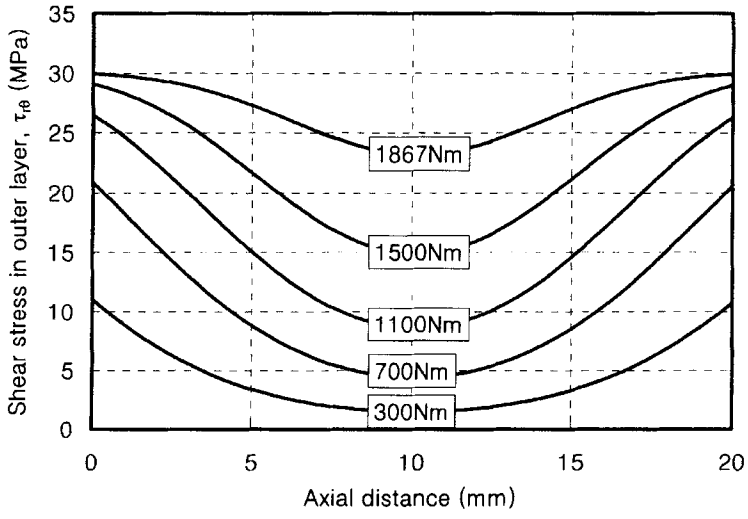

(a)

FIGURE 8 Shear stress distributions in the adhesive w.r.t. the applied torque when the joint has the configuration with the maximum torque transmission capability and the thickness of the adherend 1 is 3 mm: (a) Outer layer of the tubular double-lap joint, (b) Inner layer of the tubular double-lap joint.

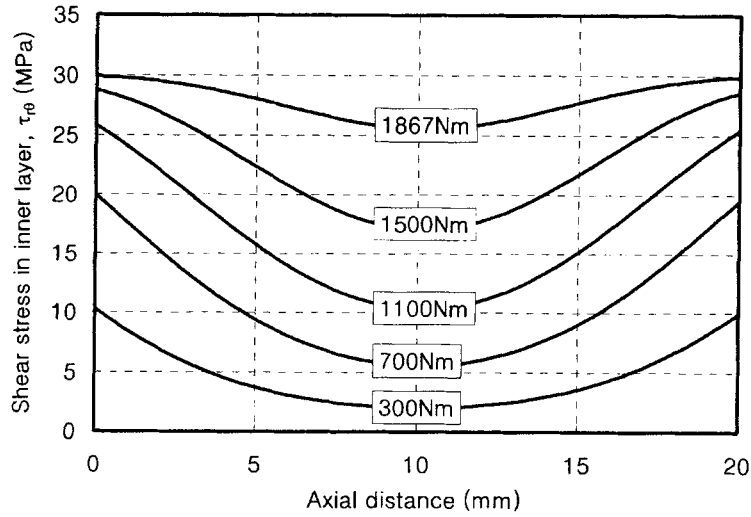

(b)

FIGURE 8 (Continued).

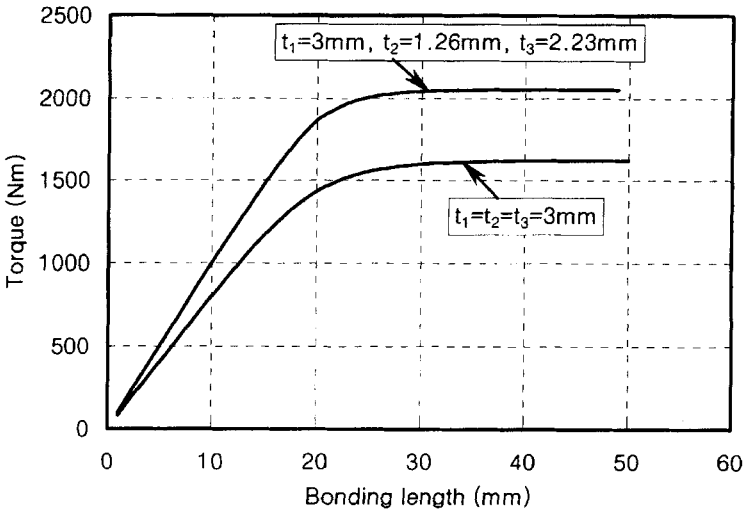

FIGURE 9 Torque transmission capabilities of the adhesively bonded tubular double-lap joint w.r.t. bonding length.

3 mm for the three adherends. Through the range of bonding length, the torque transmission capability of the joint with the configuration in Table V was greater than that of the joint whose adherend thicknesses were equally 3 mm. As the bonding length increased up to 30 mm, the torque transmission capability increased, then saturated beyond the 30 mm bonding length.

CONCLUSIONS

The iterative solution for the torque transmission capability of the adhesively bonded tubular single- and the double-lap joints with nonlinear shear properties of the adhesive was derived using both the iterative solution for the adhesively bonded single-lap joint and the closed form solution of the adhesively bonded tubular double-lap joint with linear shear properties of the adhesive. The nonlinear behavior in the adhesive thickness direction was also taken into account in the derivation.

From the numerical applications of the iterative solution, it was found that the torque transmission capability of the adhesively bonded tubular double-lap joint had a higher value than that of the adhesively bonded tubular single-lap joint, and the torque transmission capability approached a constant with increasing bond length. Also, it was found that the weighting factors, which consider the nonlinearity in the thickness direction, should be used to obtained the accurate torque transmission capability.

The simplicity of the algorithm enables the torque transmission capability and the shear stress distribution to be calculated in less than ten seconds using an IBM personal computer. This algorithm is a relatively simple and useful tool for the design of adhesively bonded tubular single- and double-lap joints.

References

[1] Adams, R. D. and Peppiatt, N. A., "Stress Analysis of Adhesive Bonded Tubular Lap Joints", *J. Adhesion* **9**, 1–18 (1977).

[2] Alwar, R. S. and Nagaraja, Y. R., "Viscoelastic Analysis of an Adhesive Tubular Joint", *J. Adhesion* **8**, 79–92 (1976).

[3] Hart-Smith, L. J., "Further Developments in the Design and Analysis of Adhesive Bonded Structural Joints in Joining of Composite Materials" **ASTM STP 749**, 3–31 (1981).

[4] Thomsen, O. T. and Kildegaard, A., "Analysis of Adhesive Bonded Generally Orthotropic Circular Shells", In: *Developments in the Science and Technology of Composite Materials, Proceedings of the Fourth European Conference of Composite Materials*, pp. 723–729 (September 25–28, 1990, Stuttgart, Germany).
[5] Chon, C. T., "Analysis of Tubular Lap Joint in Torsion", *J. Composite Materials* **16**, 268–284 (1982).
[6] Hipol, P. J., "Analysis and Optimization of Tubular Lap Joint Subjected to Torsion", *J. Composite Materials* **18**, 298–311 (1984).
[7] Lee, D. G., Kim, K. S. and Lim, Y. T., "An Experimental Study of Fatigue Strength for Adhesively Bonded Tubular Single Lap Joints", *J. Adhesion* **35**, 39–53 (1991).
[8] Lee, S. J. and Lee, D. G., "Development of a Failure Model for the Adhesively Bonded Tubular Single Lap Joint", *J. Adhesion* **40**, 1–14 (1992).
[9] Lee, S. J. and Lee, D. G., "Optimal Design of the Adhesively Bonded Tubular Single Lap Joint", *J. Adhesion* **50**, 165–180 (1995).
[10] Choi, J. K. and Lee, D. G., "Torque Transmission Capabilities of Bonded Polygonal Lap Joints for Carbon Fiber Epoxy Composites", *J. Adhesion* **48**, 235–250 (1995).
[11] Lee, S. J. and Lee, D. G., "An Iterative Solution for the Torque Transmission Capability of Adhesively Bonded Tubular Single Lap Joints with Nonlinear Shear Properties", *J. Adhesion* **53**, 217–227 (1995).
[12] Choi, J. H. and Lee, D. G., "The Torque Transmission Capabilities of the Adhesively Bonded Tubular Single Lap Joint and the Double Lap Joint", *J. Adhesion* **44**, 197–212 (1994).
[13] Lee, S. J. and Lee, D. G., "A Closed-form Solution for the Torque Transmission Capability of the Adhesively Bonded Tubular Double Lap Joint", *J. Adhesion* **44**, 271–284 (1994).
[14] Lee, D. G., Jeong, K. S. and Choi, J. H., "Analysis of the Tubular Single Lap Joint with Nonlinear Adhesive Properties", *J. Adhesion* **49**, 37–56 (1995).
[15] Kim, Y. G. and Lee, D. G., "Influence of Fabrication Residual Thermal Stresses on Rubber-toughened Adhesive Tubular Single Lap Steel–Steel Joints under Tensile Load", *J. Adhesion* **65**, 163–185 (1998).
[16] Jeong, K. S., Lee, D. G. and Kwak, Y. K., "Application of Adhesive Joining Technology for Manufacturing of the Composite Flexspline for a Harmonic Drive", *J. Adhesion* **48**, 195–216 (1995).
[17] Kim, Y. G. and Lee, D. G., "Strength Analysis of Adhesively-Bonded Tubular Single Lap Steel–Steel Joints under Axial Loads Considering Residual Thermal Stresses", *J. Adhesion* **60**, 125–140 (1997).
[18] Sancaktar, E., "Constitutive Behavior and Testing of Structural Adhesives", *Applied Mechanics Reviews* **40**, 1393–1402 (1987).
[19] Jozavi, H. and Sancaktar, E., "The Effects of Cure Temperature and Time on the Stress-Whitening Behavior of Structural Adhesives. Part I. Analysis of Bulk Tensile Data", *J. Adhesion* **27**, 143–157 (1989).
[20] Sancaktar, E. and Baechtle, D. R., "The Effect of Stress Whitening on Moisture Diffusion in Thermosetting Polymers", *J. Adhesion* **42**, 65–85 (1993).